Bistability of atmospheric oxygen and the Great Oxidation Supplementary Material

1 Supplementary figure: palaeo-oxygen

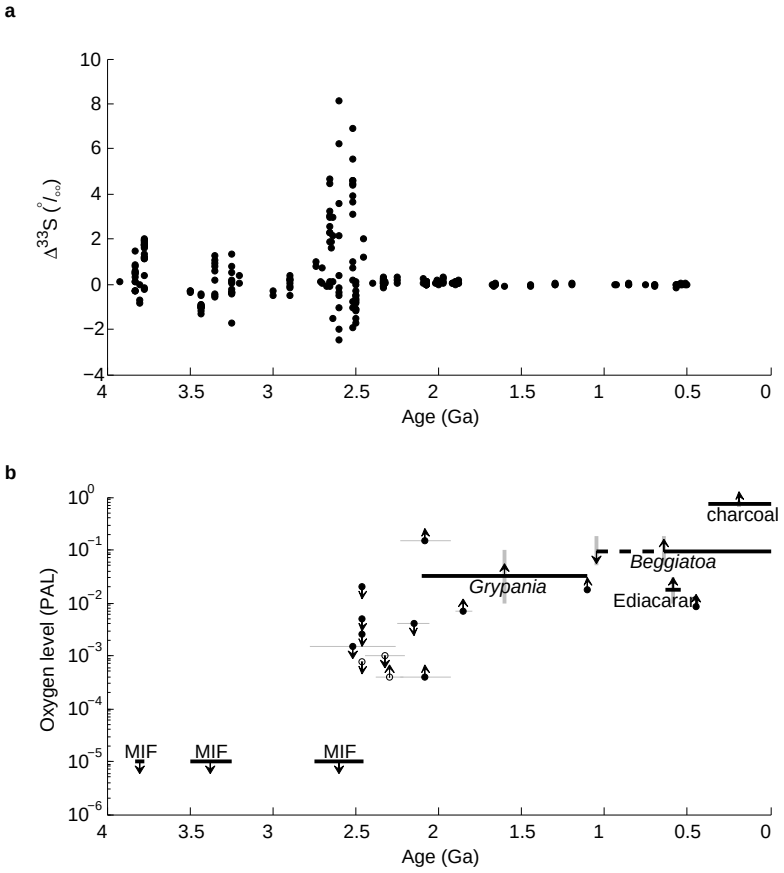

Supplementary Figure 1 — Compilation of geological evidence for Precambrian palaeo-oxygen a, Compilation of evidence of MIF in sulphur isotopes for the Precambrian[1–8]. Deviations from $\Delta^{33}S = 0$ indicate $O_2 < 10^{-5}$ PAL[9], so this strong constraint applies for the periods 3.83–3.77 Ga, 3.5–3.25 Ga and 2.75–2.45 Ga. Note the abrupt and permanent end of the strong MIF signal after 2.45 Ga. **b**, Compilation of proxy constraints on palaeo-oxygen. Upward arrow indicates lower bounds and downward arrows indicate upper bounds. Solid black lines are duration of the constraint. Dashed black line means that oxygen is thought to have crossed the given threshold in that time. Grey lines are error bars. Circles represent palaeosols[10]. The oxygen constraint for these is from an $O_2 : CO_2$ ratio and assumed pCO_2; these constraint would be affected by any change from the assumed pCO_2. Open circles are weakly constrained. Ediacaran is a constraint from the oxygen demand of fauna of that period[11]. Beggiatoa refers to oxygen constraints from

this organism together with changes in the sulphur cycle[12]. Charcoal requires sufficient oxygen for combustion[13].

2 Model derivation

Introduction The algebraic derivation of our model is given here; see the *Methods* section for a general description. The model consists of reservoirs of $\mathrm{CH_4}$ and $\mathrm{O_2}$ in the surface system (atmosphere and ocean mixed layer) and of buried organic carbon, taken as $\mathrm{CH_2O}$, in the crust. These are represented $\boldsymbol{M}$, $\boldsymbol{O}$ and $\boldsymbol{C}$ respectively with the dimension mol. For each component of the model, fluxes are calculated between the reservoirs in mol yr^{-1}; these fluxes are summed to give differential equations for each reservoir.

Boundary fluxes We are concerned with the oxidation state of the surface (atmosphere and ocean) system so a fundamental part of our model is accounting for how reductants enter or leave the system. At the top of the atmosphere, reductant can be lost in the form of hydrogen escaping to space. At the interface with the geosphere, reductants can be transferred between the surface system and the crust and mantle.

Hydrogen escape is taken to be diffusion limited so depends on the mixing ratio of methane. The net stoicheiometry is $\mathrm{CH_4} + \mathrm{O_2} + h\nu \longrightarrow 4\mathrm{H}(\uparrow \text{ space}) + \mathrm{CO_2}$ (see *Methods*) so this process is a sink of an equal number of moles of oxygen and methane. Assuming that the molar volume of the atmosphere is constant, we can scale a constant[14] $s = 2.03 \times 10^{-5}$ such that

$$\begin{aligned} \boldsymbol{M}'_{H-esc} &= -s\boldsymbol{M} \\ \boldsymbol{O}'_{H-esc} &= -s\boldsymbol{M} \end{aligned}$$

Burial and weathering of organic carbon are resolved explicitly, as described in *marine biosphere* and *weathering of buried organic carbon* sections below.

To make our model as simple as possible, we combine the remaining boundary fluxes into a single net flux, r, which is set as a boundary condition. This can include direct input from the mantle at mid-ocean ridges and weathering of inorganic reductants in the crust. Reducing power may be lost to the mantle at subduction zones. This will be a small fraction of the material which enters trenches, as most is recycled through back arc volcanism. The magnitude of this flux is very difficult to estimate even for the modern system[15]. To attempt to explicitly resolve this would be appropriate in a detailed model of the global redox system; in our minimal model such loss of reductant is simply considered to decrease the value of r.

Marine biosphere The net productivity of the biosphere is described by the assumed net productivity from oxygenic photosynthesis, N, plus the input of inorganic reductant, r, which is assumed to be an electron donor for anoxygenic photosynthesis. An assumed fraction β of the available organic carbon is buried, then a fraction, γ, is used by heterotrophic aerobic respiration (depending on available oxygen) and the remainder is used by fermenters and methanogens. Some fraction, δ, of the methane produced is oxidised by methanotrophs, depending on available oxygen. In reality, the carbon burial will be the material left *after* the action of decomposers. However, resolving the oxygen dependence of carbon burial mechanistically is beyond the scope of this paper; it would require accounting for nutrient chemistry in the ocean and whether anoxia leads to enhanced carbon burial.

In the derivation here, the change in reservoir size of each process in turn is considered. Where no flux is stated, the process has zero effect on that reservoir. For the purposes of the derivation we introduce a reservoir, $\boldsymbol{B}$, which is the amount of organic carbon available in the surface ocean, assumed to be in steady state.

1. Anoxygenic photosynthesis.
   The net input of reductant, r, is represented chemically by ferrous iron. The reducing power of this is transferred to organic carbon by anoxygenic photosynthesisers ($4\mathrm{Fe}^{2+} + \mathrm{CO}_2 + 11\mathrm{H}_2\mathrm{O} + h\nu \longrightarrow 4\mathrm{Fe(OH)}_3 + \mathrm{CH}_2\mathrm{O} + 8H^+$), so available organic carbon in the surface ocean increases.
   $$\boldsymbol{B}'_{AnoxPS} = r$$

2. Oxygenic photosynthesis.
   There is an assumed flux of oxygenic photosynthesis ($\mathrm{CO}_2 + \mathrm{H}_2\mathrm{O} + h\nu \longrightarrow \mathrm{CH}_2\mathrm{O} + \mathrm{O}_2$) represented by net primary productivity, N. This increases the availability of organic carbon in the ocean and increases the amount of oxygen in the surface system.
   $$\begin{aligned} \boldsymbol{O}'_{OxPS} &= N \\ \boldsymbol{B}'_{OxPS} &= N \end{aligned}$$

3. Organic carbon burial.
   An assumed fraction, β, of the available organic carbon in the surface ocean ($(N + r)$, contributed by both oxygenic and anoxygenic photosynthesis) is buried in sediments, reducing the amount of available organic carbon in the ocean and increasing the amount of organic carbon in the crust.
   $$\begin{aligned} \boldsymbol{C}'_{OrgCbur} &= \beta(N + r) \\ \boldsymbol{B}'_{OrgCbur} &= -\beta(N + r) \end{aligned}$$

4. Heterotrophic aerobic respiration.
   A fraction, γ, of the remaining organic carbon ($(1 - \beta)(N + r)$) in the ocean is decomposed by heterotrophic aerobic respiration ($\mathrm{CH}_2\mathrm{O} + \mathrm{O}_2 \longrightarrow \mathrm{CO}_2 + \mathrm{H}_2\mathrm{O}$). γ is a function of

oxygen; $\gamma = \boldsymbol{O}/(d_\gamma + \boldsymbol{O})$, where $d_\gamma = 1.36 \times 10^{19}$ mol, corresponding to the inhibition of aerobic respiration at the Pasteur point, $\mathrm{O_2} \sim 0.01$ PAL. This reduces the available organic carbon in the ocean and is an oxygen sink.

$$\begin{aligned} \boldsymbol{O}'_{Resp} &= -\gamma(1-\beta)(N+r) \\ \boldsymbol{B}'_{Resp} &= -\gamma(1-\beta)(N+r) \end{aligned}$$

5. Fermentors and acetogenic methanogens.
   The remainder of available organic carbon in the ocean ($(1-\gamma)(1-\beta)(N+r)$) is decomposed by anaerobic fermentors and acetogenic methanogens (summary: $2\mathrm{CH_2O} \longrightarrow \mathrm{CH_4} + \mathrm{CO_2}$). This depletes the organic carbon in the ocean and is a source of methane.

$$\begin{aligned} \boldsymbol{M}'_{Mgen} &= \tfrac{1}{2}(1-\gamma)(1-\beta)(N+r) \\ \boldsymbol{B}'_{Mgen} &= -(1-\gamma)(1-\beta)(N+r) \end{aligned}$$

6. Methanotrophs.
   A fraction, δ, of the methane produced is used by methanotrophs ($\mathrm{CH_4} + 2\mathrm{O_2} \longrightarrow \mathrm{CO_2} + 2\mathrm{H_2O}$). δ depends on oxygen; $\delta = \boldsymbol{O}/(d_\delta + \boldsymbol{O})$, where $d_\delta = 2.73 \times 10^{17}$ mol, equivalent to $[\boldsymbol{O}] = 2\ \mu$M (ref. [16]). This is a sink of both oxygen and methane.

$$\begin{aligned} \boldsymbol{M}'_{Mtroph} &= -\tfrac{1}{2}\delta(1-\gamma)(1-\beta)(N+r) \\ \boldsymbol{O}'_{Mtroph} &= -\delta(1-\gamma)(1-\beta)(N+r) \end{aligned}$$

The total effect of the biosphere is found from the summation of the above terms:

$$\begin{aligned} \boldsymbol{M}'_{bio} &= \boldsymbol{M}'_{Mgen} + \boldsymbol{M}'_{Mtroph} \\ \boldsymbol{O}'_{bio} &= \boldsymbol{O}'_{OxPS} + \boldsymbol{O}'_{Resp} + \boldsymbol{O}'_{Mtroph} \\ \boldsymbol{C}'_{bio} &= \boldsymbol{C}'_{OrgCbur} \\ \boldsymbol{B}'_{bio} &= \boldsymbol{B}'_{AnoxPS} + \boldsymbol{B}'_{OxPS} + \boldsymbol{B}'_{OrgCbur} + \boldsymbol{B}'_{Resp} + \boldsymbol{B}'_{Mgen} \end{aligned}$$

Substituting and rearranging:

$$\begin{aligned} \boldsymbol{M}'_{bio} &= \frac{1}{2}(1-\gamma)(1-\beta)(N+r) - \frac{1}{2}\delta(1-\gamma)(1-\beta)(N+r) \\ &= \frac{1}{2}(1-\delta)(1-\gamma)(1-\beta)(N+r) \\ &= \frac{1}{2}\Omega_{(\mathrm{O_2})}(1-\beta)(N+r) \end{aligned}$$

$$\begin{aligned} \boldsymbol{O}'_{bio} &= N - \gamma(1-\beta)(N+r) - \delta(1-\gamma)(1-\beta)(N+r) \\ &= (1-\gamma)(1-\delta)N - (1-(1-\gamma)(1-\delta))r + \beta(1-(1-\gamma)(1-\delta))(N+r) \\ &= \Omega_{(\mathrm{O_2})}N - (1-\Omega_{(\mathrm{O_2})})r + \beta(1-\Omega_{(\mathrm{O_2})})(N+r) \end{aligned}$$

$$
\begin{aligned}
\boldsymbol{C}'_{bio} &= \beta(N+r) \\
\\
\boldsymbol{B}'_{bio} &= r + N - \beta(N+r) - \gamma(1-\beta)(N+r) - (1-\gamma)(1-\beta)(N+r) \\
\boldsymbol{B}'_{bio} &= 0
\end{aligned}
$$

where $\Omega_{(\mathrm{O}_2)} = (1-\gamma)(1-\delta) = (1 - \frac{\boldsymbol{O}}{d_\gamma + \boldsymbol{O}})(1 - \frac{\boldsymbol{O}}{d_\delta + \boldsymbol{O}})$ is the fraction of the organic carbon available to decomposers which is transferred to the atmosphere as methane and oxygen in 1:2 balance.

In general, we use present marine net primary productivity, as our estimate for Archean net primary productivity. It has been suggested that Archean primary productivity would have been suppressed by enhanced phosphorus deposition in BIFs[17]. If this was the case, oxygen would have been lower before the Great Oxidation than is suggested in our transient runs (main article, Fig. 3). However, this removal flux of phosphorus would have ended with the cessation of BIF deposition, making present productivity a reasonable assumption for after the Great Oxidation.

Weathering of buried organic carbon We assume that the amount of buried organic carbon weathered is determined by the rate of mechanical uplift and weathering. All of the material available is assumed to be decomposed by organisms, the biochemical path depending upon oxygen availability, following the relationships established for the marine biosphere. Again, for illustrative purposes, we introduce a reservoir, $\boldsymbol{D}$, the amount of previously buried organic carbon available to decomposers, which is assumed to be in steady state.

1. Exposure of material
   Weathering processes expose buried organic carbon from the crust at assumed rate w. This reduces the amount of organic carbon in the crust and increases the amount of previously buried organic carbon available to decomposers.

$$
\begin{aligned}
\boldsymbol{C}'_{Exp} &= -w\boldsymbol{C} \\
\boldsymbol{D}'_{Exp} &= w\boldsymbol{C}
\end{aligned}
$$

2. Heterotrophic aerobic respiration
   A fraction of the available organic carbon is decomposed by heterotrophic respiration (as in the marine biosphere section), a sink of available organic carbon and of oxygen.

$$
\begin{aligned}
\boldsymbol{O}'_{Resp} &= -\gamma w\boldsymbol{C} \\
\boldsymbol{D}'_{Resp} &= -\gamma w\boldsymbol{C}
\end{aligned}
$$

3. Fermentors and acetogenic methanogens
   Remaining material is decomposed by fermentors and methanogens (as in the marine bio-

sphere section), depleting the available organic carbon and producing methane.

$$\begin{aligned} \boldsymbol{M}'_{Mgen} &= \tfrac{1}{2}(1-\gamma)w\boldsymbol{C} \\ \boldsymbol{D}'_{Mgen} &= -(1-\gamma)w\boldsymbol{C} \end{aligned}$$

4. Methanotrophs
A fraction of the methane produced is consumed by methanotrophs (as in the marine biosphere section), a sink of methane and oxygen.

$$\begin{aligned} \boldsymbol{M}'_{Mtroph} &= -\tfrac{1}{2}\delta(1-\gamma)w\boldsymbol{C} \\ \boldsymbol{O}'_{Mtroph} &= -\delta(1-\gamma)w\boldsymbol{C} \end{aligned}$$

The total effect of weathering organic carbon is found from the summation of the above terms:

$$\begin{aligned} \boldsymbol{M}'_{weath} &= \boldsymbol{M}'_{Mgen} + \boldsymbol{M}'_{Mtroph} \\ \boldsymbol{O}'_{weath} &= \boldsymbol{O}'_{Resp} + \boldsymbol{O}'_{Mtroph} \\ \boldsymbol{C}'_{weath} &= \boldsymbol{C}'_{Exp} \\ \boldsymbol{D}'_{weath} &= \boldsymbol{D}'_{Exp} + \boldsymbol{D}'_{Resp} + \boldsymbol{D}'_{Mgen} \end{aligned}$$

Substituting and rearranging:

$$\begin{aligned} \boldsymbol{M}'_{weath} &= \frac{1}{2}(1-\gamma)w\boldsymbol{C} - \frac{1}{2}\delta(1-\gamma)w\boldsymbol{C} \\ &= \frac{1}{2}(1-\delta)(1-\gamma)w\boldsymbol{C} \\ &= \frac{1}{2}\Omega_{(\mathrm{O_2})}w\boldsymbol{C} \end{aligned}$$

$$\begin{aligned} \boldsymbol{O}'_{weath} &= -\gamma w\boldsymbol{C} - \delta(1-\gamma)w\boldsymbol{C} \\ &= -(1-(1-\gamma)(1-\delta))w\boldsymbol{C} \\ &= -(1-\Omega_{(\mathrm{O_2})})w\boldsymbol{C} \end{aligned}$$

$$\boldsymbol{C}'_{weath} = -w\boldsymbol{C}$$

$$\begin{aligned} \boldsymbol{D}'_{weath} &= w\boldsymbol{C} - \gamma w\boldsymbol{C} - (1-\gamma)w\boldsymbol{C} \\ \boldsymbol{D}'_{weath} &= 0 \end{aligned}$$

w is set by analogy to present conditions; the buried organic carbon reservoir is in steady state today, $\beta(N+r) = w\boldsymbol{C}$. With $\boldsymbol{C} = 1.66 \times 10^{21}$ mol and $\beta(N+r) = 1 \times 10^{13}$ mol yr^{-1}(ref. [18]), $w = 6 \times 10^{-9}$ yr^{-1}.

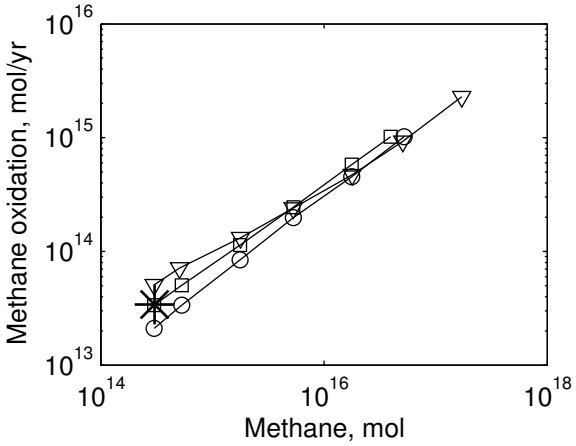

Supplementary Figure 2 — Methane oxidation rate against methane. Present observed methane oxidation flux ($*$, ref [22]) and results of photochemical model[21] for 1 PAL (∇), 0.1 PAL ($\circ$) and 0.01 PAL ($\square$).

Atmospheric methane oxidation The stoicheiometry of methane oxidation can be summarised

$$\mathrm{CH_4} + 2\mathrm{O_2} \longrightarrow \mathrm{CO_2} + 2\mathrm{H_2O}$$

but the reaction can take place by various pathways in a number of steps. The rate of the reaction depends not only on the concentration of reductants, but also on OH concentration and the degree of UV shielding (largely by ozone; we neglect the case of UV shielding by photochemical haze[19] as we envisage $[\mathrm{CH_4}] \ll [\mathrm{CO_2}]$ so no such haze should form). The influence of these additional factors depends on methane and oxygen abundances, but the relationships are complex and non-linear. Resolving these reactions requires a detailed photochemical model. Our approach is to base our parametrisation for methane oxidation on the results of such models[19–21]. In essence, this parametrisation allows us to use off-line calculations of the methane oxidation rate in our models, taking advantage of the detail in the photochemical model but maintaining conceptual simplicity and numerical efficiency in our model.

Supplementary Figure 2 shows the relationship of the model methane oxidation flux to methane abundance at various oxygen levels. The results are approximately fitted by a power law in methane concentration; Oxidation rate $\propto \boldsymbol{M}^n$ where $n \approx \{0.58, 0.75, 0.70\}$ for $\boldsymbol{O} = \{1, 0.1, 0.01\}$ PAL. In our model, we use $n = 0.7$. For present oxygen, n is not constant with respect to $\boldsymbol{M}$, but is approximately 0.7 for realistic methane levels.

Supplementary Figure 3 shows the methane oxidation flux, corrected for the relationship with methane derived above, against oxygen abundance. A polynomial is fitted to the data; $\log(\mathrm{oxidation}/\boldsymbol{M}^{0.7}) = a_1\psi^4 + a_2\psi^3 + a_3\psi^2 + a_4\psi + a_5$ where $\psi = \log \boldsymbol{O}$, $a_1 = 0.0030$, $a_2 = -0.1655$, $a_3 = 3.2305$,

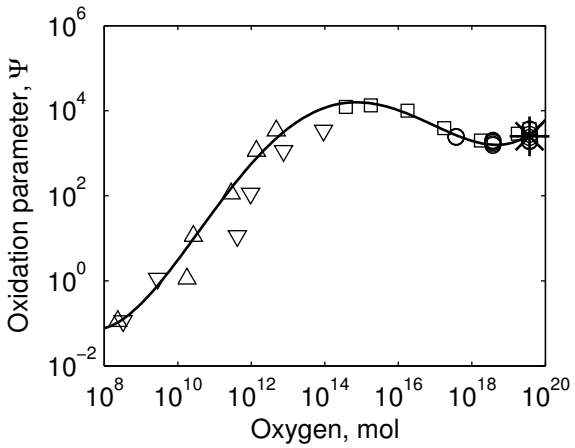

Supplementary Figure 3 — Methane oxidation against oxygen, corrected for methane level. $\Psi = \mathrm{oxidation}/\boldsymbol{M}^{0.7}$. Present observed methane oxidation flux ($*$, ref [22]) and data from various photochemical models ($\triangle$, ref. [19] without haze; ∇ ref. [19] with haze; $\square$ ref. [20]; $\circ$ ref. [21]).

$a_4 = -25.8343$ and $a_5 = 71.5398$, valid for $10^8 < \boldsymbol{O} < 10^{20}$ mol. Where $\boldsymbol{O} < 10^{14}$, the fit approximates to a straight line with $\mathrm{d}\log(\mathrm{oxidation})/\mathrm{d}\boldsymbol{M} = 1$; a linear dependence of oxidation flux on oxygen. If there was no effect of UV shielding one would envisage extrapolating this line to higher oxygen levels. However, at these higher oxygen levels an ozone layer develops[23] which suppresses the effective rate of oxidation.

Thus, with $\Psi_{(\mathrm{O}_2)} = 10^{a_1\psi^4+a_2\psi^3+a_3\psi^2+a_4\psi+a_5}$ we have

$$\begin{aligned} \boldsymbol{M}'_{MethOx} &= -\frac{1}{2}\Psi_{(\mathrm{O}_2)}\boldsymbol{M}^{0.7} \\ \boldsymbol{O}'_{MethOx} &= -\Psi_{(\mathrm{O}_2)}\boldsymbol{M}^{0.7} \end{aligned}$$

Full model The model is the summation of the above terms

$$\begin{aligned} \boldsymbol{M}' &= \boldsymbol{M}'_{bio} + \boldsymbol{M}'_{weath} + \boldsymbol{M}'_{H-esc} + \boldsymbol{M}'_{MethOx} \\ \boldsymbol{O}' &= \boldsymbol{O}'_{bio} + \boldsymbol{O}'_{weath} + \boldsymbol{O}'_{H-esc} + \boldsymbol{O}'_{MethOx} \\ \boldsymbol{C}' &= \boldsymbol{C}'_{bio} + \boldsymbol{C}'_{weath} \end{aligned}$$

Substituting and rearranging:

$$\begin{aligned} \boldsymbol{M}' &= \frac{1}{2}\Omega_{(\mathrm{O}_2)}(1-\beta)(N+r) + \frac{1}{2}\Omega_{(\mathrm{O}_2)}w\boldsymbol{C} - s\boldsymbol{M} - \frac{1}{2}\Psi_{(\mathrm{O}_2)}\boldsymbol{M}^{0.7} \\ &= \frac{1}{2}\Omega_{(\mathrm{O}_2)}(N+r) - s\boldsymbol{M} - \frac{1}{2}\Psi_{(\mathrm{O}_2)}\boldsymbol{M}^{0.7} - \frac{1}{2}\Omega_{(\mathrm{O}_2)}(\beta(N+r) - w\boldsymbol{C}) \end{aligned} \quad (1)$$

$$
\begin{aligned}
\boldsymbol{O'} &= \Omega_{(O_2)}N - (1-\Omega_{(O_2)})r + \beta(1-\Omega_{(O_2)})(N+r) - (1-\Omega_{(O_2)})w\boldsymbol{C} - s\boldsymbol{M} - \Psi_{(O_2)}\boldsymbol{M}^{0.7} \\
&= \Omega_{(O_2)}N - (1-\Omega_{(O_2)})r - s\boldsymbol{M} - \Psi_{(O_2)}\boldsymbol{M}^{0.7} + (1-\Omega_{(O_2)})(\beta(N+r) - w\boldsymbol{C}) \qquad (2)
\end{aligned}
$$

$$
\boldsymbol{C'} = \beta(N+r) - w\boldsymbol{C} \qquad (3)
$$

Steady state solutions The steady state solutions of the model are found by setting Eqs. 1 – 3 to zero:

$$
\begin{aligned}
0 &= \frac{1}{2}\Omega_{(O_2)}(N+r) - s\boldsymbol{M} - \frac{1}{2}\Psi_{(O_2)}\boldsymbol{M}^{0.7} - \frac{1}{2}\Omega_{(O_2)}(\beta(N+r) - w\boldsymbol{C}) \qquad (4) \\
0 &= \Omega_{(O_2)}N - (1-\Omega_{(O_2)})r - s\boldsymbol{M} - \Psi_{(O_2)}\boldsymbol{M}^{0.7} + (1-\Omega_{(O_2)})(\beta(N+r) - w\boldsymbol{C}) \qquad (5) \\
0 &= \beta(N+r) - w\boldsymbol{C} \qquad (6)
\end{aligned}
$$

Eq. 3 states that in steady state, burial and weathering of organic carbon are equal. Thus we get the steady state solution for buried organic carbon,

$$
\boldsymbol{C} = \frac{\beta(N+r)}{w} \qquad (7)
$$

Substituting into Eqs. 1 – 2,

$$
\begin{aligned}
0 &= \frac{1}{2}\Omega_{(O_2)}(N+r) - s\boldsymbol{M} - \frac{1}{2}\Psi_{(O_2)}\boldsymbol{M}^{0.7} - \frac{1}{2}\Omega_{(O_2)}\left(\beta(N+r) - w\frac{\beta(N+r)}{w}\right) \\
&= \frac{1}{2}\Omega_{(O_2)}(N+r) - s\boldsymbol{M} - \frac{1}{2}\Psi_{(O_2)}\boldsymbol{M}^{0.7} \qquad (8) \\
0 &= \Omega_{(O_2)}N - (1-\Omega_{(O_2)})r - s\boldsymbol{M} - \Psi_{(O_2)}\boldsymbol{M}^{0.7} + (1-\Omega_{(O_2)})\left(\beta(N+r) - w\frac{\beta(N+r)}{w}\right) \\
&= \Omega_{(O_2)}N - (1-\Omega_{(O_2)})r - s\boldsymbol{M} - \Psi_{(O_2)}\boldsymbol{M}^{0.7} \qquad (9)
\end{aligned}
$$

$2 \times (\text{Eq.}8) - (\text{Eq.}9)$ gives

$$
0 = r - s\boldsymbol{M} \qquad (10)
$$

This shows that reductant input to the surface system is balanced by hydrogen loss to space. Hence the steady state solution for methane which gives this balance is

$$
\boldsymbol{M} = \frac{r}{s} \qquad (11)
$$

Substituting in Eq. 8

$$
\begin{aligned}
0 &= \frac{1}{2}\Omega_{(O_2)}(N+r) - s\left(\frac{r}{s}\right) - \frac{1}{2}\Psi_{(O_2)}\left(\frac{r}{s}\right)^{0.7} \\
&= \Omega_{(O_2)}N + (\Omega_{(O_2)} - 2)r - \Psi_{(O_2)}\left(\frac{r}{s}\right)^{0.7} \qquad (12)
\end{aligned}
$$

Steady state oxygen is found by solving Eq. 12 numerically, recalling the nonlinear dependencies of $\Omega_{(O_2)}$ and $\Psi_{(O_2)}$ on oxygen abundance.

Simplified steady state solutions Once oxygenic photosynthesis is established, $N \gg r$ and $\Omega_{(\mathrm{O}_2)}N \approx \Psi_{(\mathrm{O}_2)}\left(\frac{r}{s}\right)^{0.7} \gg (\Omega_{(\mathrm{O}_2)} - 2)r$. Hence we can state a simplified steady state equation for oxygen

$$0 = \Omega_{(\mathrm{O}_2)}N - \Psi_{(\mathrm{O}_2)}\left(\frac{r}{s}\right)^{0.7} \tag{13}$$

This equation shows that, for steady state conditions when oxygenic photosynthesis is well established, the amount of oxygen in the atmosphere adjusts such that loss oxidising methane balances the net production from the biota. This is valid when atmospheric oxygen exceeds 1×10^9 PAL. Similarly, the steady state solution for buried organic carbon becomes

$$\boldsymbol{C} = \frac{\beta N}{w} \tag{14}$$

3 Temperature difference calculation

We do not resolve carbon dioxide concentrations, so we cannot calculate actual temperatures. However, using results from an ensemble of radiative–convective climate model results (Figure 1 and Equation 1 of ref. [24]), it can be seen that the temperature *difference* due to a change in methane concentration is largely independent of carbon dioxide concentration. For changes in methane concentration over multi-million year time periods, carbon dioxide concentrations will adjust due to negative feedback in the carbonate–silicate cycle[25]. However, for changes in methane concentration much faster than the response time of the carbonate–silicate cycle, temperature difference estimates are valid.

1. Farquhar, J., Bao, H. & Thiemens, M. Atmospheric influence of Earth's earliest sulfur cycle. *Science* **289**, 757–758 (2000).

2. Ono, S. *et al.* New insights into Archean sulfur cycle from mass-independent sulfur isotope records from the hamersley basin, australia. *Earth Planet. Sci. Lett.* **213**, 15–30 (2003).

3. Hu, G., Rumble, D. & Wang, P.-L. An ultraviolet laser microprobe for the in situ analysis of multisulfur isotopes and its use in measuring Archean sulfur isotope mass-independent anomalies. *Geochim. Cosmochim. Acta* **67**, 3101–3117 (2003).

4. Mojzsis, S., Coath, C., Greenwood, J., McKeegan, K. & Harrison, T. Mass-independent isotope effects in Archean (2.5 to 3.8 Ga) sedimentary sulfides determined by ion microprobe analysis. *Geochim. Cosmochim. Acta* **67**, 1635–1658 (2003).

5. Bekker, A. *et al.* Dating the rise of atmospheric oxygen. *Nature* **427**, 117–120 (2004).

6. Johnston, D. *et al.* Active microbial sulfur disproportionation in the Mesoproterozoic. *Scinece* **310**, 1477–1479 (2005).

7. Papineau, D., Mojzsis, S., Coath, C., Karhu, J. & McKeegan, K. Multiple sulfur isotopes of sulfides from sediments in the aftermath of Paleoproterozoic glaciations. *Geochim. Cosmochim. Acta* **69**, 5033–5060 (2005).

8. Ono, S., Beukes, N., Rumble, D. & Fogel, M. Early evolution of atmospheric oxygen from multiple-sulfur and carbon isotope records of the 2.9 Ga Mozaan group of the Pongola supergroup, southern Africa. *S. Afr. J. Geol* (In press).

9. Pavlov, A. A., Kasting, J. F., Brown, L. L., Rages, K. A. & Freedman, R. Greenhouse warming by CH_4 in the atmosphere of early Earth. *J. Geophys. Res* **105**, 11,981–11,990 (2000).

10. Rye, R. & D., H. H. Paleosols and the evolution of atmospheric oxygen: A critical review. *Am. J. Sci.* **298**, 621–672 (1998).

11. Runnegar, B. Precambrian oxygen levels estimated from biochemistry and physiology of early eukaryotes. *Palaeogeogr. Palaeocl.* **97**, 97–111 (1991).

12. Canfield, D. & Teske, A. Late Proterozoic rise in atmospheric oxygen concentration infered from phylogenetic and sulphur isotope studies. *Nature* **382**, 127–132 (1996).

13. Rowe, N. & Jones, T. Devonian charcoal. *Palaeogeogr. Palaeocl.* **164**, 331–338 (2000).

14. Catling, D., Zahnle, K. & McKay, C. Biogenic methane, hydrogen escape, and the irreversible oxidation of early Earth. *Science* **293**, 839–843 (2001).

15. Hayes, J. M. & Waldbauer, J. R. The carbon cycle and associated redox processed through time. *Philos. T. Roy. Soc. B* **361**, 931–950 (2006).

16. Ren, T., Amaral, J. A. & Knowles, R. The response of methane consumption by pure cultures of methanotropic bacteria to oxygen. *Can. J. Microbiol* **43**, 925–928 (1997).

17. Bjerrum, C. & Canfield, D. Ocean productivity before about 1.9 Gyr ago limited by phosphorus adsorption onto iron oxides. *Nature* **417**, 159–162 (2002).

18. Holland, H. D. *The chemistry of the atmosphere and oceans* (Wiley, New York, 1978).

19. Pavlov, A., Brown, L. & Kasting, J. UV shielding of NH_3 and O_2 by organic hazes in the Archean atmosphere. *J. Geophys. Res* **106**, 23267–23287 (2001).

20. Pavlov, A. & Kasting, J. Mass-indeependent fractionation of sulfur isotopes in Archean sediments: strong evidence for and anoxic Archean atmosphere. *Astrobiology* **2**, 27–41 (2002).

21. Pavlov, A., Hurtgen, M., Kasting, J. & Arthur, M. Methane-rich Proterozoic atmosphere? *Geology* **31**, 87–90 (2003).

22. Prather, N. *et al.* Atmospheric chemistry and greenhouse gasses. In Houghton, J. *et al.* (eds.) *Climate Change 2001: The Scientific Basis. Contribution of working group I to the Third Assesment Report of the Intergovernmental Panel on Climate Change.* (Cambridge University Press, Cantab., U.K., 2001).

23. Kasting, J. & Donahue, T. The evolution of the atmospheric ozone. *J. Geophys. Res* **85**, 3255–3263 (1980).

24. Kasting, J., Pavlov, A. & Siefert, J. A coupled ecosystem–climate model for prediction the methane concentration of in the Archean atmosphere. *Origins Life Evol. Biosphere* **31**, 271–285 (2001).

25. Walker, J., Hays, P. & Kasting, J. A negative feedback mechanism for the long-term stabilisation of the Earth's surface temperature. *J. Geophys. Res* **86**, 9776–9782 (1981).